PARAMETRIC EFFECTS ON SPOILER GEOMETRY ASSESSMENT WITH CHIMERA TECHNIQUE

X. Bertrand
Airbus
316 route de Bayonne 31060 Toulouse Cedex 9, France

1. ABSTRACT

This paper presents the use of CFD methods based on RANS equations and Chimera technique to simulate the flow on a transport aircraft with deployed spoilers to improve the physical understanding of these control surfaces.

The first part of the paper explains spoiler aerodynamics and their interactions with the wings, HTP and VTP. Then, spoiler geometry is modified as a function of various parameters (position on wing span and chord, hinge line sweep, spoiler chord size) and the impact of these geometrical effects on handling qualities coefficients is detailed.

2. INTRODUCTION

Prediction of spoiler effectiveness and hinge moment is an important part of the aircraft sizing process, as these devices have a significant impact on handling qualities and final aircraft weight. The flowfield of a wing with deflected spoiler is complex, with massive separation, possible reattachment and vortex shedding, making the study of this control surface very difficult to simulate with CFD. Until recently, only costly wind tunnel tests and semi-empirical methods (SEM) with limited accuracy were employed to model spoiler effectiveness of Airbus aircraft.

Spoilers are first sized thanks to SEM, based on Airbus experience on previous aircraft. SEM are very fast and they provide good results in many cases, if these cases are not too different from existing aircraft. Nevertheless, SEM accuracy is limited, and the physical understanding of the phenomenon can be further improved. Consequently, some margins have to be considered, to ensure the handling qualities of the aircraft in all cases. These margins increase the aircraft weight, on the one hand directly through the spoiler size, and on the other hand by requiring bigger actuators.

The next step is to test a representative model in a wind tunnel to determine more precisely the spoiler effectiveness, in order to create Aerodynamic Data. Because of the significant cost of each wind tunnel model, and the required manufacturing lead-time to build it, it is very difficult to improve spoiler-sizing relying only on wind tunnel tests. Consequently, there is an opportunity to optimize the sizing of spoilers and actuators compared to the past.

Several studies (see [4] & [6] for example) have been realized to determine the flow around an airfoil with a deflected spoiler through numerical computations. While the 2D physical phenomena appears to be well known, the limited number of 3D studies (see [1], [2], [3], & [5]) suggests the physical understanding of the flow around a wing with deployed spoilers is quite restricted.

CFD has been used at Airbus for a long time for shape design and optimization. With the recent progress in numerical simulations, involving automatic mesh generation and a wide use of the Chimera technique (see [8] and [9]), CFD is more and more used to generate Aerodynamic Data, including aileron and spoiler effectiveness. The capability of elsA to compute configurations with deflected spoilers was studied by Fillola et al. ([1] & [2]) demonstrating the accuracy of elsA with Chimera meshes to determine spoiler effectiveness for Aerodynamic Data, by comparison with wind tunnel tests. This study also emphasized the interactions between Horizontal and Vertical Tail Planes (HTP & VTP) and spoiler wake, and the necessity to simulate asymmetrical aircraft to calculate rolling moment, because of interactions between left and right wings.

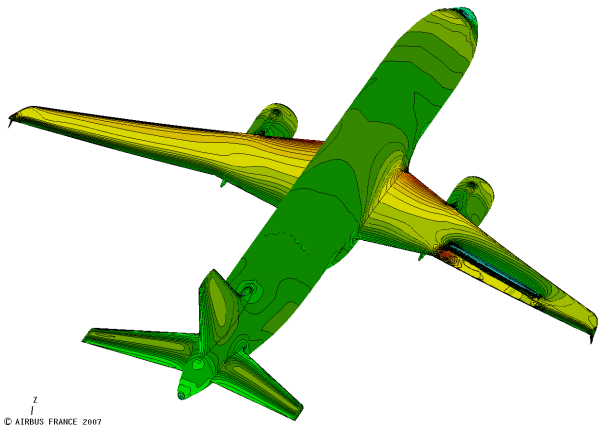

FIG. 1: Cp curves on a single aisle aircraft with deflected spoiler at M=0.5 α=2°, δsp=30°. The spoiler is modelled thanks to a Chimera overset mesh.

The Chimera approach is revealed to be extremely interesting because it enables easy & quick modelling of aircraft with deployed spoilers and allows to improve the physical understanding of the associated flow features. In this paper, several basic effects on spoiler layout have been identified, such as spoiler size and position. This has been investigated through application on a classical Airbus aircraft with conventional HTP and VTP. The objective is to provide

a physical analysis of the flow behaviour according to the considered effect in order to ease the configuration optimization.

3. NUMERICAL METHODS

The numerical analysis has been realized with the *elsA* (see [7]) solver, developed by ONERA, CERFACS and Airbus. *ElsA* is an object-oriented solver, for structured multiblocks and multigrid meshes. The main interest of *elsA* for this study is its ability to treat Chimera overset meshes, which is useful for moveable surface applications.

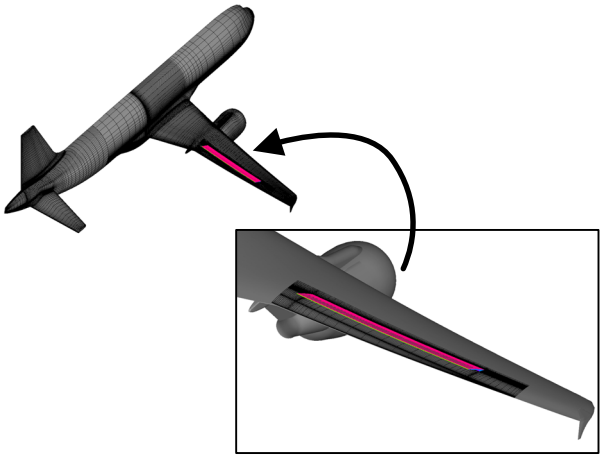

FIG. 2: Chimera mesh overset for spoiler

A global aircraft mesh with deflected spoiler can be decomposed into two domains:

- Aircraft mesh
- Spoiler mesh (generated with an automatic mesher)

The aircraft mesh is the same for all calculated cases and only new spoiler meshes have to be generated. Fillola has validated this approach by comparison of CFD calculations with wind tunnel tests, in order to generate data for handling qualities. There was a good agreement between wind tunnel test results and his calculations for DCz, DCx, DCl and DCm, with and without HTP/VTP.

This paper, based on the results of this previous study, assumes that elsA with Chimera mesh for spoiler deflection represents an appropriate means to model the airflow, and can give accurate data easily

The aircraft mesh represents a classical single aisle aircraft, with HTP (setting angle i_H=-0.82°), VTP, wing tip fences, nacelle and pylon. There are 4M nodes in this mesh, and approximately 1M in the spoiler mesh.

The turbulence model used is the Airbus standard model Spalart-Allmaras. All calculations have been carried out by applying a multigrid method with two levels, with both angle of attack and sideslip at 0°. The Mach number is 0.5, with a Reynolds number of 29.10^6.

DCz, DCx and DCm are calculated on a symmetrical mesh (spoilers deflected on both wings), whereas DCl is calculated on a asymmetrical mesh with spoiler deflected on right wing only, in order to take into account interaction between left and right wings (see §4.2).

4. SPOILER PHYSICS

4.1. Spoiler aerodynamics

Even if spoilers/airbrakes have different applications (lift dumping, emergency descent, roll control, load alleviation…), the goal of these surfaces is globally to increase aircraft drag and to decrease lift through a massive separation on the upper wing.

Pressure in front of the deflected surface rises, and shockwaves move upstream at transonic Mach number. The flow separates behind the spoiler, dividing the pressure distribution in three zones with positive and negative lift (FIG. 3), with a massive impact on wing loads distribution (FIG. 5). Wing lift is then completely destroyed, and thanks to the flow separation behind the spoiler, drag is widely increased.

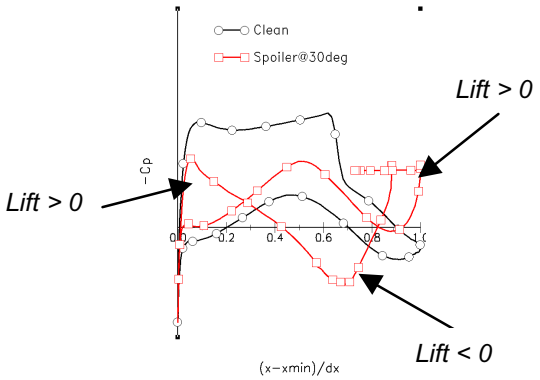

FIG. 3: Pressure distribution on wing with and without deployed spoilers at y/b=0.55, M=0.8, α=2°, δsp=20°

The huge negative lift zone at mid-profile with a deployed spoiler increases wing pitching moment calculated at 25% Aerodynamic Mean Chord (AMC) (FIG. 4).

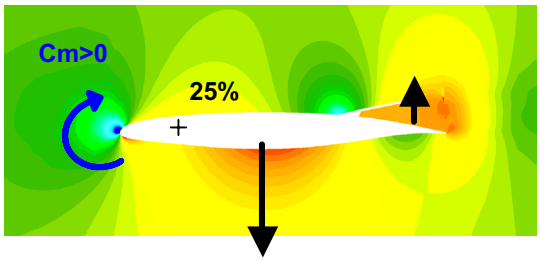

FIG. 4: Spoiler deflection creates nose-up pitching moment

4.2. Interactions

4.2.1. Left/right wing interactions

FIG. 5 shows the necessity to use asymmetrical meshes to model accurately interactions between right and left wings to calculate rolling moment. Discrepancies appear on the internal right wing between symmetrical and asymmetrical configurations. The right wing spoiler has also a small effect on the whole left wing, decreasing its lift. Finally, interactions between left and right wings are extremely important for rolling moment calculation. A full asymmetrical aircraft mesh gives more accurate results.

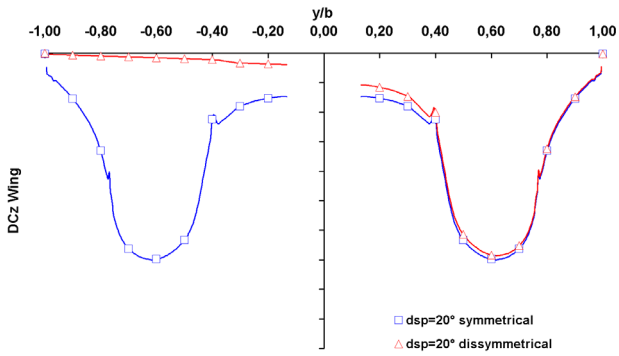

FIG. 5: Wing lift increment distribution in clean configuration and symmetrical/asymmetrical external spoiler deflection M=0.5, α=0°, δsp=20°

	Half A/C	Asymmetrical A/C
DCl	100%	92%

TAB 1: rolling moment effectiveness calculated with a asymmetrical aircraft mesh (interactions modelled) or a half aircraft mesh (no interactions between the two wings)

4.2.2. Spoiler/Tailplanes interactions

Because of loads gradient at spoiler tips (FIG. 6), two contra-rotating vortices are generated, which induce velocities on the HTP.

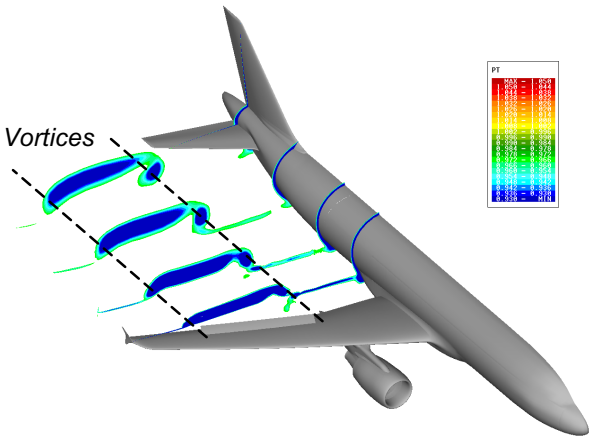

FIG. 6: The total pressure loss in the spoiler wake highlights vortices at spoiler tips

Therefore, even if the spoiler's wake does not touch directly the tailplanes, these vortices modify the local downwash ε on the HTP, and determine the main part of spoiler/horizontal tailplane interactions according to the following principle:

$$(1)\quad Cz_{HTP} = \left(\frac{\partial Cz}{\partial \alpha}\right)_{HTP} \left(\alpha_{\infty} - \varepsilon + i_H - \alpha_{0H}\right)$$

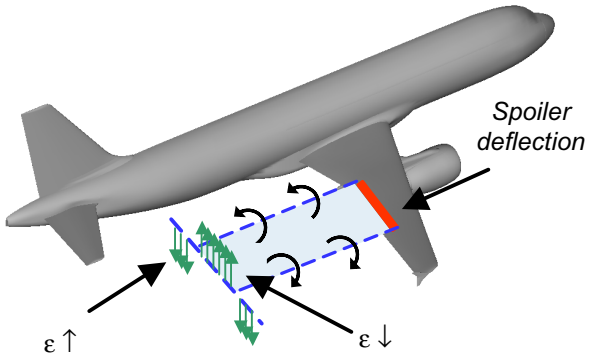

FIG. 7: Vortices trailing from spoiler tips induce vertical velocities that modify the local downwash

Consequently, the relative position of HTP and spoiler is the preponderant factor. In this study, as deflected spoilers are always external to the HTP, they increase the downwash. Hence, HTP lift is slightly reduced, which increases global aircraft lift effectiveness:

	Full A/C	Wing	HTP
DCz	100%	97%	3%

TAB 2: lift effectiveness decomposition

Nevertheless, this downwash increment on HTP reduces the drag effectiveness (FIG. 8). The projection of HTP lift in aircraft aerodynamic axis system shows a drag term along x-axis ($Cz_{HTP} \cdot \sin\varepsilon$). For negative HTP

lift and positive downwash, this drag is negative as well.

Finally, with deployed spoilers, because of downwash increment $\Delta\varepsilon$, HTP drag increment is negative, reducing spoiler drag effectiveness.

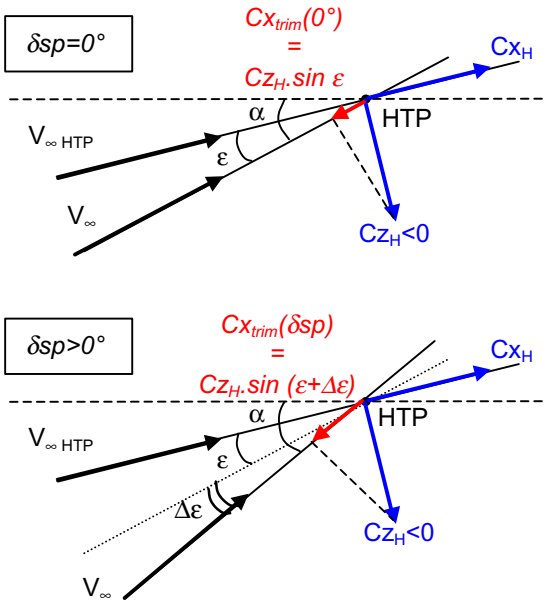

FIG. 8: Trim drag principles. Deploying spoilers increases downwash ($\Delta\varepsilon>0$), resulting in a negative trim drag increment: DCxtrim= Cxtrim(δsp)-Cxtrim(0°)<0

	Full A/C	Wing	HTP
DCx	100%	105%	-5%

TAB 3: drag effectiveness decomposition

Because of the lever arm between HTP and 25% AMC, even a small modification of HTP lift will deeply modify full aircraft pitching moment. Consequently, horizontal tailplanes represent a large contribution to spoiler Cm effectiveness.

	Full A/C	Wing	HTP
DCm	100%	70%	30%

TAB 4: pitching moment effectiveness decomposition

Therefore, for an asymmetrical deflection, right wing vortices will induce vertical velocities on both left and right HTP (FIG. 9), which will slightly contribute to rolling moment.

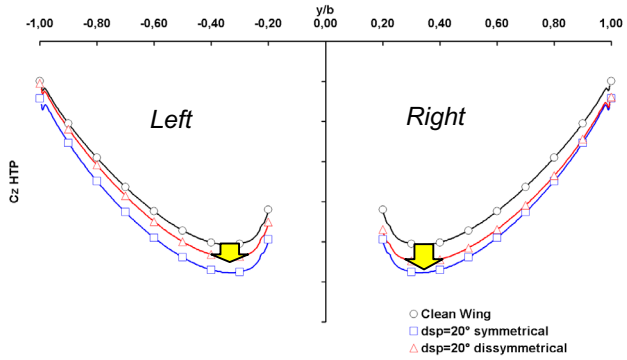

FIG. 9: HTP lift distribution in clean configuration and symmetrical/asymmetrical external spoiler deflection M=0.5, α=0°, δsp=20°.

With asymmetrical spoiler deflection, VTP is put in a sideslip field, also contributing to rolling moment (FIG. 10).

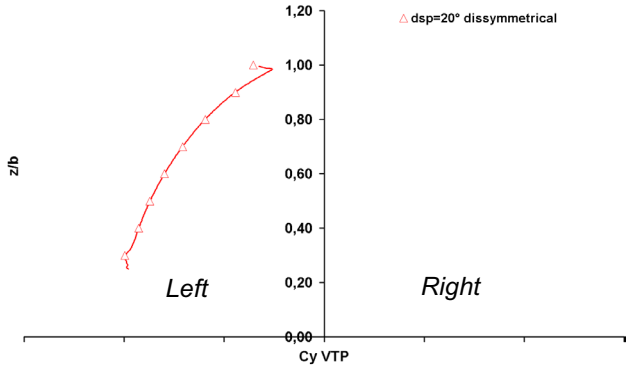

FIG. 10: VTP lateral force distribution with asymmetrical external spoiler deflection at M=0.5, α=0°, δsp=20

HTP and VTP play opposite role in rolling moment effectiveness with deployed spoilers. Their total influence is very limited, and the wings create the main part of rolling moment.

	Full A/C	Wing	HTP	VTP
DCl	100%	102%	0.5%	-2.5%

TAB 5: rolling moment decomposition

5. PARAMETRIC EFFECTS ON SPOILER GEOMETRY

5.1. Effects description

The following study aims at understanding the impact of elementary modifications on spoiler geometry. The whole study has been realized on a classical single aisle aircraft. The four external spoilers (spoiler 2, 3, 4 and 5) deflected all together at 20°, represent the reference configuration. For all the effects studied in this paper, we suppose there are four spoilers deflected

all together.

- Spoiler chord modification: the reference case is the large one. The chords of the two other cases are smaller, representing 50% and 75% of the reference chord.

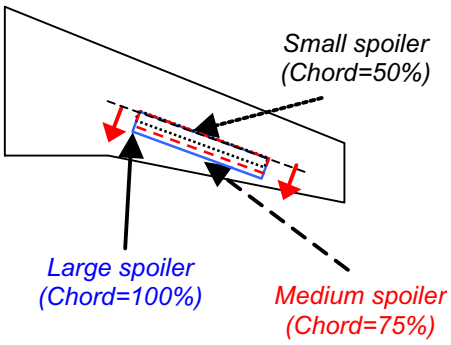

- Spoiler position along x-axis: the spoiler hinge line is moved upstream or downstream from the reference (centered) position. As the basic aircraft spoilers are quite large, the chord of all these 3 cases is taken as 50% of the reference one. Hinge line is moved by half the spoiler chord..

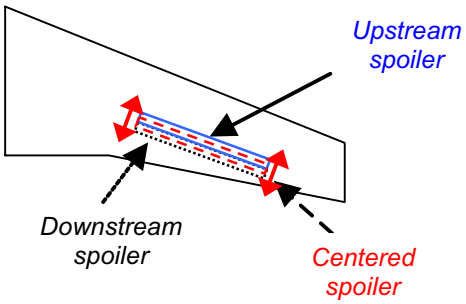

- Spoiler position along y axis: the spoiler is moved by 25% of its length in the inboard or outboard direction, with the same span and the same hinge line. The used chord is the reference one.

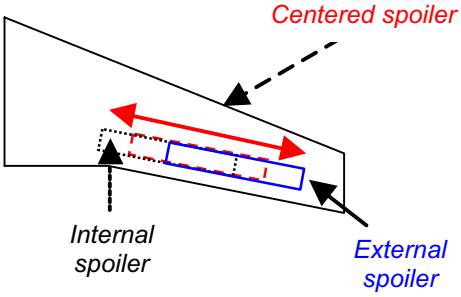

- Sweep effect of the hinge line: the spoiler hinge line sweep angle is increased or decreased by 2° steps, through a rotation around the spoiler centre.

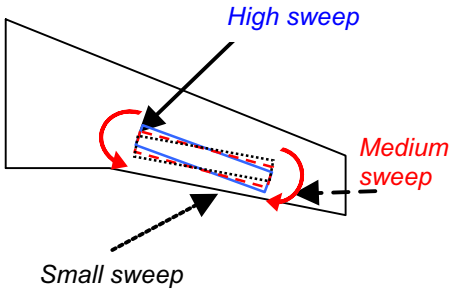

5.2. Physical analysis

5.2.1. Spoiler chord effect

First of all, spoiler chord length has little effect on lower wing pressures, whereas the separated zone behind the spoiler depends directly on this size (FIG. 11). A large spoiler naturally increases lift effectiveness: the downstream lifting zone is slightly reduced and has a huge impact on wing lift distribution (FIG. 12).

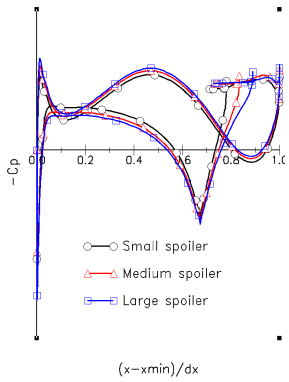

FIG. 11: Pressure distribution on wing with different spoiler chords at y/b=0.55, M=0.5, α=0°, δsp=20°

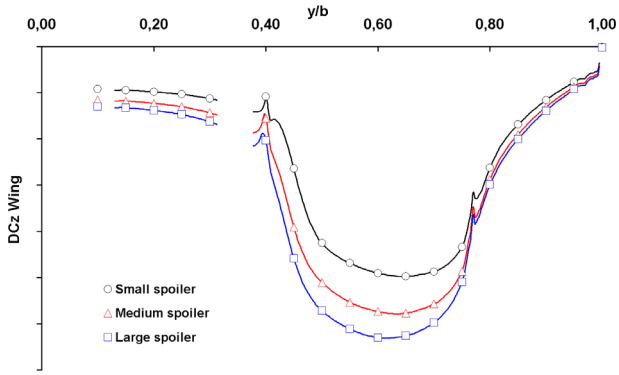

FIG. 12: Wing lift increment distribution for small, medium and large spoiler chords, M=0.5, α=0°, δsp=20°

Due to area increment, drag effectiveness grows linearly with spoiler size (FIG. 13).

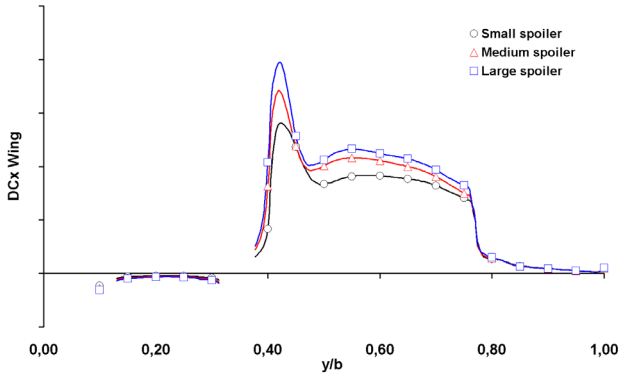

FIG. 13: Wing drag increment distribution for small, medium and large spoiler chord, M=0.5, α=0°, δsp=20°

As detailed in TAB 5, HTP and VTP represent only a small part of rolling moment effectiveness. Its main part comes from the wing, so a large spoiler is more efficient in terms of rolling moment.

Pitching moment is higher for large spoilers than for small ones: the larger lifting zone behind the small spoiler reduces the nose-up pitching moment.

Regarding hinge moment coefficient, direct comparison between the three cases is not objective because the spoiler reference surface is modified. The fairest way to compare the results is to consider the product of the reference volume and the hinge moment as directly proportional to the dimensioned torque M applied to the spoiler:

$$(1)\quad M_{spoiler} = P_{dyn} V_{spoiler} Cmc$$

$$(2)\quad V_{spoiler} = S_{spoiler} \cdot l_{spoiler} \propto l^2_{spoiler}$$

$V_{spoiler}$ is the reference volume of the considered spoiler, P_{dyn} the dynamic pressure, $S_{spoiler}$ the spoiler surface and $l_{spoiler}$ its chord length. $V_{spoiler}$ is thus proportional to the square of $l_{spoiler}$ (eq. 2).

As Cmc is more or less of the same order of magnitude with the three different chords, V*Cmc also mainly depends on the square of the chord. Therefore, reducing the spoiler chord by 25% nearly divides by two the torque applied to the actuator.

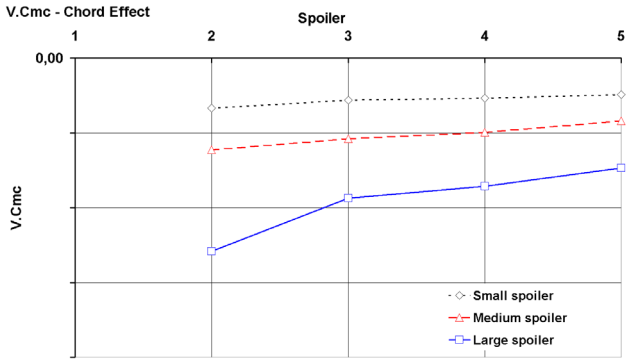

FIG. 14: product of hinge moment coefficient by reference volume of the spoiler, which is proportional to the dimensioned torque

5.2.2. Spoiler position along x axis

Shifting the spoiler hinge line position along the x-axis with constant spoiler chord, lower wing pressures are unchanged. Only upper wing pressures vary. The lift loss with an upstream spoiler (huge negative lift zone in front of it) is balanced by lift creation behind the surface. Finally, the global wing lift is the same in the three cases, and FIG. 16 highlights the limited discrepancies between the three calculated cases.

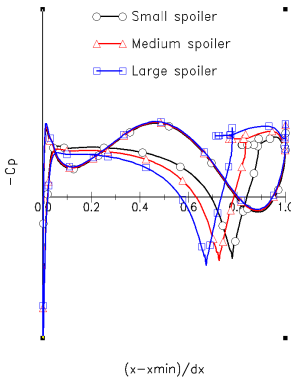

FIG. 15: Pressure distribution on the wing at y/b=0.55 for 3 positions of the spoiler

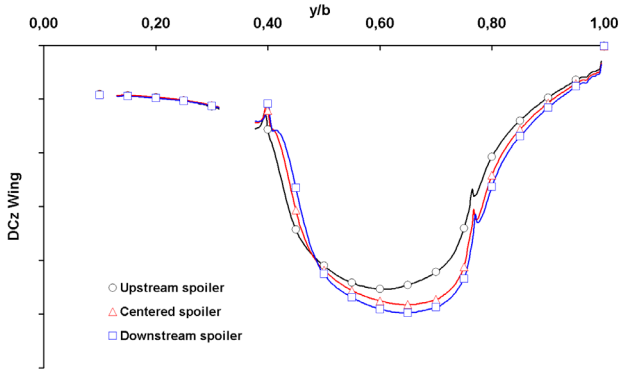

FIG. 16: Wing lift increment distribution for upstream, centered and downstream spoilers, M=0.5, α=0°, δsp=20°

DCx depends linearly on this effect. An upstream spoiler will create more drag than a downstream spoiler, because of higher pressure differences around the surface (FIG. 17).

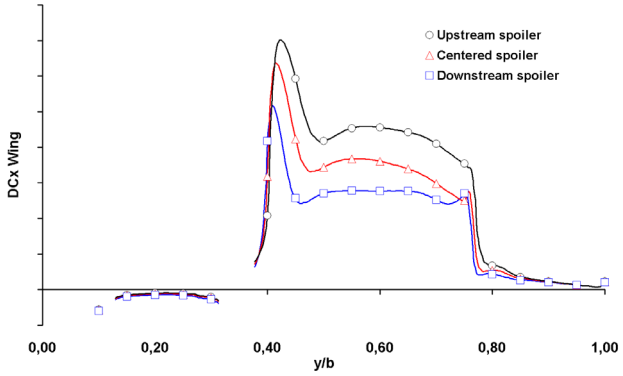

FIG. 17: Wing drag increment distribution for upstream, centered and downstream spoilers, M=0.5, α=0°, δsp=20°

It is the same phenomenon for Cmc: the more the spoiler upstream, the higher the hinge moment.

This geometrical effect does not modify pitch and rolling moment effectiveness. Vortices intensity do not vary, so spoiler/tailplane interactions are the same in the three cases.

5.2.3. Spoiler position along y-axis

We saw in §4.2 that spoiler/HTP interactions mainly depend on their relative position along y-axis: downwash value evolves. This has therefore many consequences on lift, drag and pitching moment.

First of all, we can consider an aircraft without tailplanes. As drag mainly depends on spoiler area, it is not changed by spoiler position along y-axis. However, an internal spoiler has a better lift effectiveness than an external spoiler.

Thanks to a higher lever arm external spoiler has better rolling moment effectiveness than internal spoilers. Due to wing sweep angle, the external spoiler is further from the reference point for pitching moment calculation (25% AMC). Therefore, external spoiler increases DCm on an isolated wing.

FIG. 18 shows that spoiler/HTP interactions are completely different in the three cases. Contrary to internal spoiler, external and centered spoiler vortices do not intersect HTP. Thus, internal spoiler will not increase downwash on the whole HTP span.

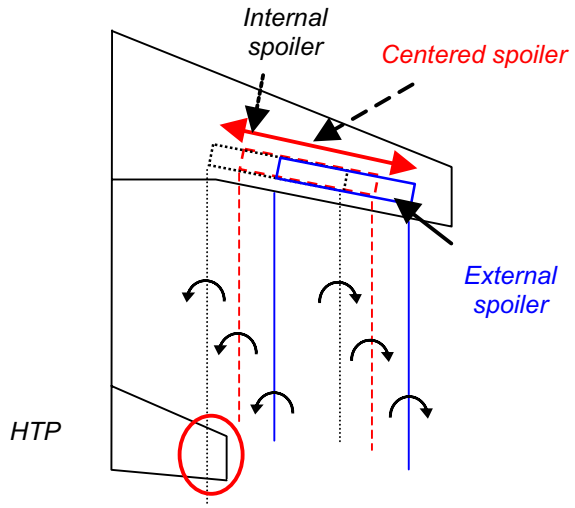

FIG. 18: Simplified representation of vortices position for position along y-axis effect. Inner vortex of internal case intersects HTP

This causes the lift increment on the HTP to vary with the y-position of the spoiler, which is evidenced in FIG. 19, showing a downwash increment or decrement.

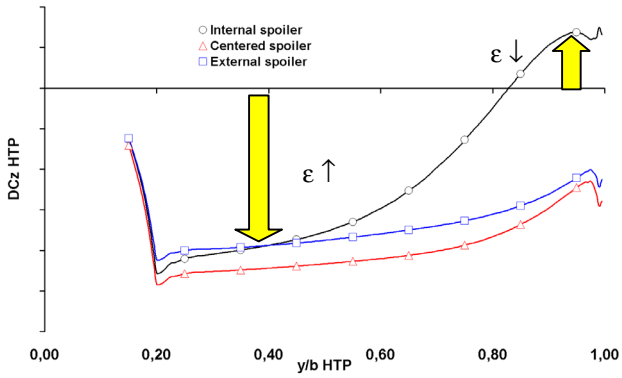

FIG. 19: HTP lift increment distribution for inner, centered and outer spoiler. Inner case creates positive and negative downwash

Internal spoiler has a smaller impact on HTP lift than the other cases, and consequently smaller pitching moment effectiveness.

5.2.4. Spoiler sweep effect

An analysis of pressure distributions at three different sections of the wing (internal, medium and external spoiler span) shows that spoiler sweep effect can be explained only by considering the spoiler hinge line position on wing profile. A spoiler with a small sweep will have its internal side further downstream than a spoiler with a high sweep angle, and the opposite for the external side. Finally, pressure distributions are locally very similar to those found when considering the effect of varying the position along x-axis (FIG. 20). Sweep effect might be regarded as a simple change of spoiler local position on the wing chord.

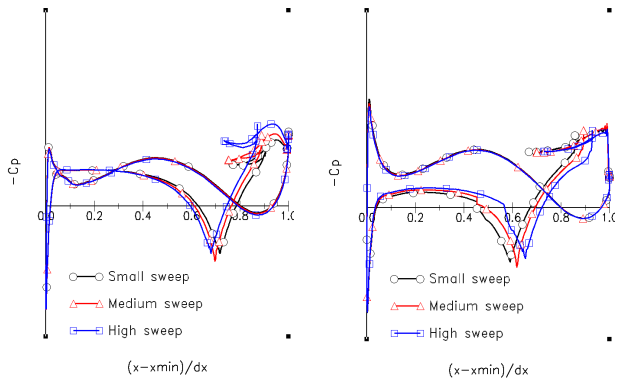

FIG. 20: Pressure distribution at y/b=45%, and 75%

Therefore, increasing spoiler sweep angle has not much effect on the spoiler lift effectiveness, while this sweep increment remains small (FIG. 21). On the studied case, a small sweep angle is a little more efficient than a high one. This observation probably depends on wing and spoiler geometry, and it is certainly dangerous to extend this remark to other aircraft. With different spoiler chord, other wing planform or another reference point for the rotation the tendencies would probably be different.

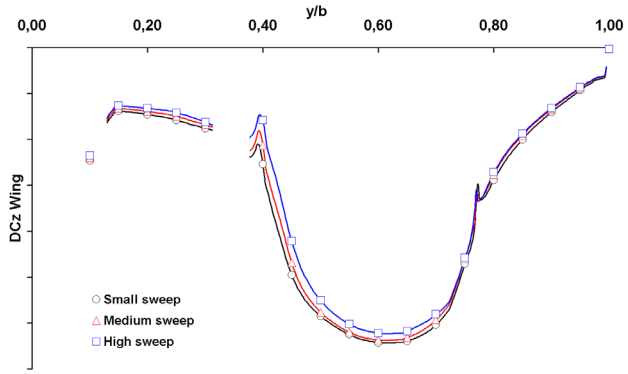

FIG. 21: Wing lift increment distribution for small, medium and large hinge line sweep angle, M=0.5, α=0°, δsp=20°

Drag increment distribution (FIG. 22) emphasizes the equivalence sweep effect/position along x-axis. The most important drag on internal side is obtained with a high sweep spoiler, whereas on external side it is obtained with small sweep spoiler.

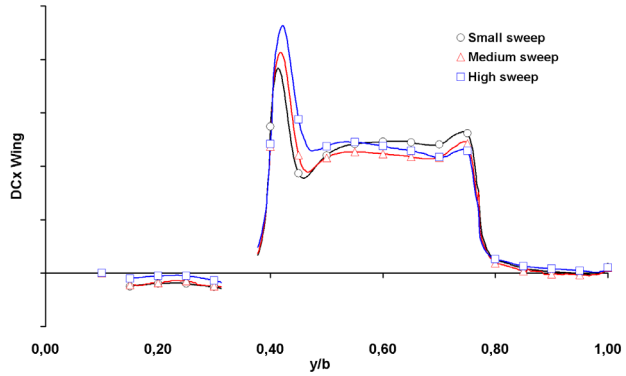

FIG. 22: Wing drag increment distribution for small, medium and large hinge line sweep angle, M=0.5, α=0°, δsp=20°

Because of the limited effect on wing load distribution of hinge line sweep, pitching and rolling moments do not vary a lot.

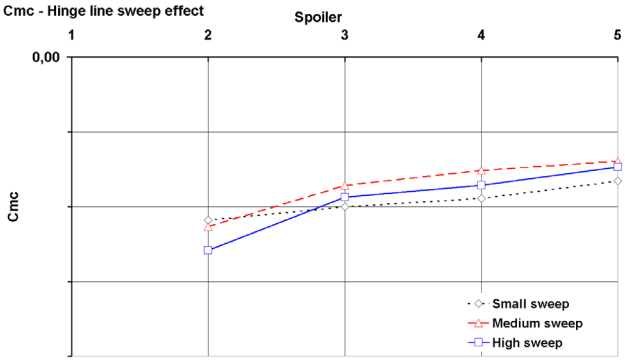

FIG. 23: Hinge moment coefficient for small, medium and high spoiler sweep angle.

Nevertheless, the hinge line sweep effect seems to have an important impact on Cmc (FIG. 23). High sweep angle generates low pressure levels behind spoiler 2, implying high Cmc for this particular spoiler. Reducing the sweep angle limits the hinge moment of this spoiler, even if it increases the ones of the other spoiler.

6. CONCLUSION

The complexity of the flow, with massive separated zones, on an aircraft with deployed spoilers was a severe constraint for handling qualities quantification. Wind tunnel tests were mandatory to estimate accurately the effectiveness of this kind of control surfaces, with an important cost and limited optimisation possible during aircraft development. Thanks to Chimera meshing technique, CFD computations on an aircraft with deflected airbrakes are affordable, and moreover they have an excellent accuracy.

A great advantage is the improvement of the physical understanding of spoiler aerodynamics: interactions

with the tailplanes in symmetrical and asymmetrical configuration have been explained.

Then, a database of effects on spoiler geometry has been calculated for the purpose of configuration optimisation. The main tendencies have been explained and can be used for back-to-back assessments.

Nowadays, the interest of the Chimera technique for the prediction of handling qualities of an aircraft is clear. The methodology described in this paper can be extended to all the others moveable surfaces such as ailerons, rudder and elevator with the same advantages and accuracy.

7. REFERENCE

[1] Fillola, G., Carrier, G., Dor, J-B, “Experimental Study and Numerical Simulation of Flow Around Wing Control Surface”, ICAS 2006 Hamburg
[2] Fillola, G., Le Pape, M-C., Montagnac, M., “Numerical Simulations Around Wing Control Surfaces”, ICAS 2004, Yokohama
[3] Mertins, R., Barakat, S., Elsholz, E., “3D viscous flow simulation on spoiler and flap configuration”; German Aerospace Congress 2003, Munich
[4] Al-Bahi, A., “Investigation of the Flow Field Past an Airfoil-Spoiler Configuration”, AIAA 1996, Reno
[5] Tinoco, E., Bogue, D., Kao, T-J., Li, P, Ball, D., “Progress Toward CFD for Full Flight Enveloppe”, Aeronautical Journal Volume 109, October 2005
[6] Costes, M, “Comparison Between Experimental and Computational Results for Airfoils Equipped with a Spoiler and a Flap”, AIAA 1985, Colorado Springs
[7] Gazaix, M., Jolles, A., Lazareff, M., ”The elsA Object Oriented Computation Tool for Industrial Applications”, ICAS 2002, Toronto
[8] Jeanfaivre G., Benoît, Ch., Le Pape, M-C., “Improvement of the Robustness of the Chimera Method’, AIAA paper, 02-3290, St Louis, June 2002
[9] Steger, J-L., Dougherty, F-C., Benek J-A., “A Chimera grid Scheme”, in Advance in Grid Generation, K.N. Ghia and U. Ghia, eds, ASME FED, Vol. 5 pp56-69, 1983